Letters in Applied NanoBioScience
Open-Access Journal (ISSN: 2284-6808)

Article
Volume 15, Issue 2, 2026, 58
https://doi.org/10.33263/LIANBS152.058

Designing Microbial Fuel Cells (MFCs) Including *Geothrix fermentans* and *Gluconobacter oxydans* Bacteria: Invistegation with Numerical Analysis

Majid Monajjemi [1,*], Fatemeh Mollaamin [2], Samira Mohammadi [3], Yasamin Shahverdy [3], Mersedeh Rahpayma [4,5]

[1] Department of Biology, Faculty of Science, Kastamonu University, Kastamonu, Turkey
[2] Department of Biomedical Engineering, Faculty of Engineering and Architecture, Kastamonu University, Kastamonu, Turkey
[3] Department of Chemical Engineering, CT.C., Islamic Azad University, Tehran, Iran
[4] Department of Fundamental Science, Faculty of Pharmaceutical Science, Medical Science Branch, Islamic Azad University, Tehran, Iran
[5] Department of Dentistry, Faculty of Dentistry, Kocaeli Health and Technology University, Kocaeli, Turkey
* Correspondence: mmonajjemi@kastamonu.edu.tr;

Received: 14.07.2025; Accepted: 28.02.2026; Published: 30.06.2026

Abstract: In this work, we exhibited the effect of temperature and also cell dimensions on the microbial fuel cells (MFCs) efficiency according to our experimental data. In other words, microbial fuel cells (MFCs) are emerging as promising technologies for applications such as electricity generation. Electroactive (EA) biofilms formed by microorganisms play a central role in bioelectrochemical systems through microbially mediated electrocatalytic reactions. In this study, industrial wastewater containing *Geothrix fermentans* and *Gluconobacter oxydans* was evaluated for power generation in MFCs. The effects of temperature, reactor configuration, chamber dimensions, and the distance between anodic and cathodic electrodes on electrical output were systematically investigated. Statistical analyses, including descriptive statistics, correlation, and regression, were performed using SPSS to predict average voltage from the derived regression model. A two-dimensional model was further employed to analyze ionic transport, the distribution of electronic current density, and local reaction rates in both anodic and cathodic chambers. Two types of bacteria were examined: the anaerobic *Geothrix fermentans*, known for its ability to utilize Fe(III) and other high-potential metals as electron acceptors, and the aerobic *Gluconobacter oxydans*, tested in a miniature MFC (mini-MFC) system. The results indicated that the aerobic mini-MFC achieved a lower maximum power output than the anaerobic system. Additionally, numerical fitting was performed for MFCs operating under varying temperatures and chamber dimensions. The numerical results showed strong agreement with experimental data, confirming the validity of the proposed model.

Keywords: oxydans bacteria; *Geothrix* and *Gluconobacter*; microbial fuel cell (MFC); sustainable energy source; waste materials; electroactive (EA) biofilms; bioelectrochemical systems.

1. Introduction

1.1. MFCs as a novel technology.

A microbial fuel cell (MFC) utilizes the growth and metabolic activities of microorganisms, such as exoelectrogenic bacteria, to directly convert the chemical energy. The flux continuity condition (Eq. 11) was applied at the biofilm–analyte interface, assuming the presence of a concentration boundary layer with a thickness of *L*. The flux continuity condition (Eq. 11) was applied at the biofilm–analyte interface, assuming the presence of a concentration boundary layer with a thickness of *L*. stored in organic waste into electricity [1]. In recent years, the generation of renewable energy from wastewater effluents containing active microorganisms has been widely investigated as a clean and sustainable alternative to petroleum-based energy sources [1–4]. In this context, bioelectrochemical systems based on MFC technology represent a novel and promising approach for producing electricity from wastewater while contributing to global efforts to mitigate climate change [3,4]. These technologies enable the direct conversion of chemical energy in waste materials into electrical energy, thereby helping to reduce greenhouse gas emissions and environmental pollution [5]. In MFCs, electrochemical reactions occur at solid conductive electrodes, where organic pollutants serve as substrate fuels. Waste effluents act as feed sources for microorganisms during cellular respiration, leading to electron transfer from microbial cells to the electrode surface [6].

Microbial involvement in the electrochemical mechanism enhances catalytic activity and facilitates electron-transfer processes. In this work, we investigated the optimization of pollutant removal and electricity generation through the design of a laboratory-scale modeling system incorporating nanomaterials in the electrode structure. Improving the interaction between the bacterial external cell membrane and the electrode surface using nanomaterials can reduce internal resistance and enhance power output during bioelectricity generation. Nanocomposites such as CNT/MnO_2 were selected based on their superior electrocatalytic properties, thermal and chemical stability, biocompatibility, high surface-area-to-volume ratio, and favorable electron-transfer characteristics for simultaneous energy harvesting and pollutant removal [7]. These properties significantly enhance electrical performance by accelerating electron-transfer rates in electrochemical reactions [7].

One of the primary objectives of this study is to identify suitable nanomaterials for efficient energy recovery from various types of microbial waste [8]. The presence of electroactive microorganisms in waste-rich effluents, particularly in large urban areas, offers substantial potential for sustainable clean energy production and environmental protection [9]. Furthermore, the degradation of chemical substrates using multifunctional nanomaterials in conjunction with electroactive microorganisms represents an effective strategy for simultaneous wastewater treatment and electricity generation.

The continuous consumption of fossil fuels not only depletes natural resources but also increases CO_2 emissions, thereby accelerating global warming [10]. Therefore, integrating waste management with MFC technology presents a sustainable and renewable energy solution in commercial and environmental sectors [11,12].

In this study, a two-dimensional mathematical model was developed to analyze process-parameter relationships quantitatively and to provide deeper insight into the effect of temperature on MFC performance. The model predictions were validated using experimental data obtained from a single-chamber, air-cathode MFC. Additionally, the effects of electrode

spacing and ionic strength were investigated to demonstrate the broader applicability and robustness of the proposed mathematical model.

1.2. MFC model.

A microbial fuel cell basically contains an anode chamber, a cathode chamber, a PEM or salt bridge, an external circuit, and an electrode assembly. Many different configurations are used in MFCs. The most common configuration is a two-chamber MFC with an "H" shape, consisting of two bottles connected by a tube with a proton exchange membrane in the middle. The key point of this design is the use of a small membrane separating the two chambers. However, these MFCs typically have a high internal resistance due to the long distance between the two electrodes and the membrane's small surface area, thereby limiting power density. Two-chamber MFCs are basically used in batch mode and can also run in continuous mode [13]. The electrons move from the anode to the cathode through the external circuit, whereas protons move through the salt bridge, which is known as a proton exchange membrane (PEM). Reduction occurs at the cathode in the presence of oxygen, and the protons form water in the cathodic chamber. Hence, the bacteria form CO_2 and H_2O during the decomposition of substrate, and therefore, because of oxygen's role as an inhibitor, the anode chambers should be made Anaerobic. Since the anode chamber is anaerobic and the cathode chamber can be aerobic, the cathode electrode can be omitted, resulting in a single-compartment MFC.

For instance, using acetate as a substrate, the cathodic and anodic reactions are as follows.

$$\text{Anodic reaction: } C_2H_4O_2+2H_2O \rightarrow 2CO_2 + 8e^- + 8H^+ \quad (1)$$

$$\text{Cathodic reaction: } 2O_2+8e^- + 8H^+ \rightarrow 4H_2O \quad (2)$$

The performance of MFC can be estimated through the power density parameter and the intensity of electrical current. Since MFC is a function of many variables, multidisciplinary subjects and various fields would require the best optimization. In this work for the MFC model, we focused mostly on nano materials of electrodes, substrates, and various electrogenic microorganisms. The best bioremediation can be achieved with Gram-negative bacteria, which, due to unique phospholipid structures in their cell membranes, facilitate the degradation of organic waste products [14,15].

Although bacteria degrade hazardous organic substances through metabolic reactions, some compounds, such as halogenated aromatic hydrocarbons, exhibit high resistance to microbial attack during these reactions [15,16]. Because of bacteria's capability of transferring electron potential and forming a slimy layer biofilm, they are known as electrochemically active bacteria (EAB). EAB is a novel subject for converting the chemical energy to electrical energy through bioremediation technology [17]. Biofilms are communities of electroactive microorganisms that are preserved by extracellular compounds, including polysaccharides, proteins, and nucleic acids, located outside the cells of the microorganisms. These biofilms increase the conducting electrode with surfaces of bacterial cell attachment [18].

Because microbes harbor hazardous molecules, bacteria can degrade waste compounds to obtain energy and a carbon source to survive in their life cycle [19]. *Gluconobacter oxydans* and *Geothrix fermentans* can produce electrons within the cell and then transfer them to extracellular acceptors via cytochromes and biofilms. These batteries exhibit sufficient columbic performance as acceptors in biofilms on the electrode surface and can transfer electrons directly to the anode, thereby increasing energy production [20].

2. Materials and Methods

2.1. MFC systems.

Our MFC system (Figure 1) is made of 1- Anode chamber that keep the bacteria and organic substrate in an anaerobic media, 2- Cathode chamber that keep a conductive solution of salt, 3- Salt bridge including Proton-exchange membrane for separating the anode and cathode chambers from each other but enable to transit the protons from anodic chamber to cathodic chamber, and 4- External circuit for transit the electrons towards cathode chamber as well as a path for electrons for pulling out from the anode. Bacteria, during oxidation as part of their metabolic activity, produce protons and electrons that are pulled out of solution at the anode through circuit wires and deposited on a related electrode, and then the electrons are conducted into the cathode chamber. Since MFC is powered through various bacteria in the anode chamber, we selected two important bacteria, including *Gluconobacter oxydans* and *Geothrix fermentans*. Obviously, the electronic power production is dependent on various agents such as the type of bacteria, organic material, which the bacteria enable to digest, temperature, and concentration of bacteria per anode chamber volume unit.

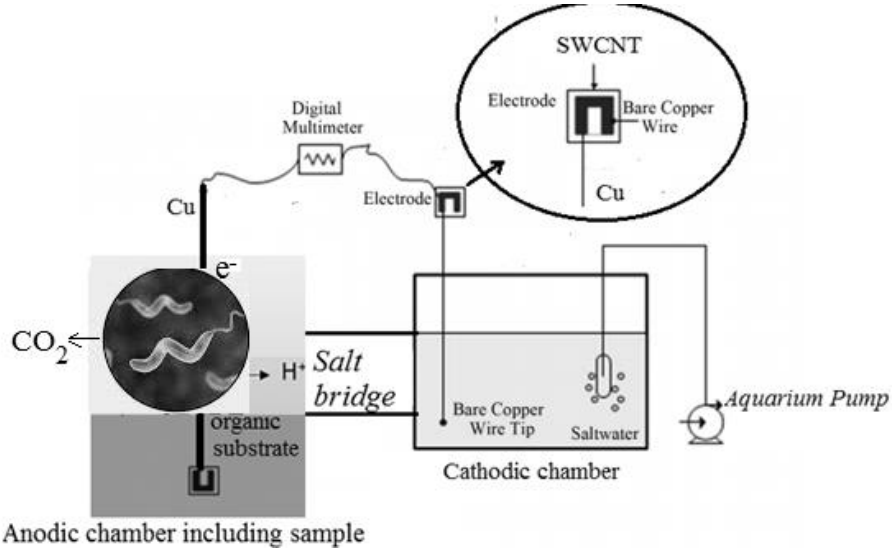

Figure 1. Schematic of MFC system setup, including anodic and cathodic chambers containing SWCNT electrode.

2.2. Membrane selection.

Membranes in MFCs have a basic character due to the decreasing internal resistance, prevention of pH splitting, and saving costs. It is notable that membrane compounds are generally categorized as cation exchange membrane (CEM), anion exchange membrane (AEM), and we checked and tested any of these types in our experiments [21]. The most commonly applicable membrane is CEM, which is widely used due to its easy proton transfer. We tested both Nafion 115 and Ultrex CMI 7000 and confirmed Nafion 115 because the negatively charged hydrophilic sulfonate group attached to hydrophobic fluorocarbon has the most efficiency in CEM cerise. We also selected Nafion 115 commercial membranes (Dupont Company) in the Na^+-form (Nafion-Na) with dimensions of 100× 30 × 0.125 mm. The Nafion-Na membranes exhibited ionic conductivity of 3.52×10^{-4} S cm−1 at 298 K and 1.52×10^{-3} S cm^{-1} at 70 °C, respectively [22]. Based on Koók *et al.*'s work, we also connected the cathode chamber to the membrane section for removing impurities and increasing the porosity of the

membrane [23]. Before starting the tests, Nafion was prepared by using 5 wt% hydrogen peroxide and 15 wt% sulfuric acid at 80°C for one hour, respectively. The sodium-ion exchange procedure was mixed in 250 ml of NaOH aqueous solution (10 g sodium hydroxide in 250 ml of de-ionized water) at 80°C for 5 h [21- 23]. Since CEM cerise has a major drawback for using CEM in MFC in long-term operations, in other experiments, we used AEM. We showed that the AEM series exhibits an excellent proton transfer rate compared with CEM, owing to the phosphate or carbonate structure. In addition, pH is better balanced in MFC with AEM because of phosphate anions [24]. Table 1 presents a summary of various membranes, and we used Tokuyama: A201 Tokuyama's AEM products from Japan among this list [25-30].

Table 1. A summary of various membranes.

Membrane	**Backbones**	**Transferring Functional group**	**Membrane specification (a):Ionic conductivity;(b):IEC; (c)Thickness; (d):Tensile strength; (e): Elongation at break**
Tokuyama: A201 and A901	-	-	(a) 42 mS cm $^{-1}$ (OH^-); (b)1.8 meq/g; (c) 28 µm; (d) 96 Mpa; (e) 62%
Aemion™ series	Methylated polybenzimidazoles	Imidazole	(a)80 mS cm $^{-1}$; (b)2.1–2.5 meq/g; (c) Depends on the Product chosen; (d) 60MPa; (e) 80-110%
XION™Composite-72-10CL	Poly-norbornene	Pendant quaternary ammonium	(c) 10 µm; (d) No; (a) No; (d) No
PiperION™ Versogene	Poly-aryl Piperidinium	PiPeridine	(a) 150 mS cm^{-1} (OH^-); (b) 1.04meq/g; (c) Depends on the Product chosen;(d) Tensile strength: >30 MPa; (e) Elongation at break>30%
aQAPS-S8	Polysulfon	quaternary ammonium	(a) 54 mS cm^{-1} (OH^-); (b) 1.8 meq/g; (c) 50 µm, (d) No:, (e) No
Orion TM1	Poly-terphenylen	Pendant quaternary ammonium	(a) 54 mS cm^{-1} (OH^-); I(b) 2.19 meq/g; (c) 24 µm; (d) 30 MPa; (e) 35%

2.3. Preparation of anode chamber.

The anodic chamber is a major part, where decomposition of biomass is done inside this electrode for creating the initial bacterial activity. The performance of an MFC is typically described by measuring the anode efficiency, as it serves as an active center for living bioelectrochemical activities and as a mediator of electron transport from exoelectrogens to the anodic chamber. Therefore, it is essential to concentrate on the anode materials and design. Several items influence the performance of the MFC, such as bio materials in anodic chambers, bacteria types, and proton transfer membranes. Usually, carbonaceous metal-based compounds are widely used in MFCs, such as carbon paper, carbon rods, carbonized cardboard, and carbon cloth, the last of which is used in the anodic chamber due to its high strength and high porosity, which create a relatively high surface area [31-35]. Carbon paper combined with multi-walled carbon nanotubes (MWCNTs) through a layer-by-layer assembly technique was used as a suitable electrode in an anodic chamber.

This type of modification reduces interfacial charge transfer by providing three-dimensional network structures for bacterial adhesion, resulting in 20% higher power densities than an unmodified carbon cloth electrode. In this work, we used both types of carbon cloth as electrodes, which were soaked in distilled water at 298 K for half an hour and then boiled in deionized water for 15 minutes to remove contaminants accumulated within their pores. Three layers of carbon cloth cover the T-shaped anode to achieve an appropriate thickness. We also used several metal plates, mostly stainless steel sheets, for anode materials.

2.4. Preparation of cathode chamber.

In the cathodic chamber, the electrons reduce oxygen to water through reduction reactions, which can occur at the three-phase interface among air, liquid, and solid. A general cathodic chamber electrode consists of an electrode assist, a special catalyst, and an air diffusion section. Although anodic chamber electrode materials can sometimes be used in cathodic chambers, it is notable that the cathode material should have higher conductivity and mechanical strength than anodic materials. Mostly MFCs are being worked under neutral PH and mild temperatures. Although by these amounts the rate of oxygen reduction is not quick enough to increase over potentials, for strong reactions in the cathodic chamber, the cathodic carbon-based support materials must be amended with additional catalysts. Using expensive transition metals such as platinum, gold, and even silver as catalysts for cathode materials is limiting the practical applications of MFC technology. Therefore, it is necessary to reduce the cost of cathodic catalysts by replacing platinum with cheaper materials, such as carbon cloth coated with polytetrafluoroethylene, without sacrificing efficiency. The MFC efficiency by using carbon cloth coated with poly-tetrafluoroethylene increased the power densities by around 35% compared with a carbon-based cloth one-layered. Recently, it has been confirmed that four layers of polytetrafluoroethylene produced the maximum power density because this combination reduces water losses through the cathode. In this work, we used commercial carbon electrodes due to properties like a wide electrochemical window, low residual current, recyclability, reusability, and sufficient electrical conductivity. Despite graphite, cathode chamber materials could be similar to anode chamber materials, such as cloth, rods, and paper carbon combined with some cheaper transition metals, including nickel and titanium [36]. In our work, we used a combination platinum-carbon catalyst on the cathode chamber electrode to increase the rate of oxygen recovery and reduce the overpotential at the cathode. Thus, platinum powder with a 15 wt% loading of 0.20 mg/, water, and ethanol was mixed for half an hour.

Next, 50 wt% of the ordinary polymer binder in the fabrication of metal-carbon composite electrodes, polytetrafluoroethylene (PTFE), was added to make a 40 wt% solution, and the mixture was stirred for 15 minutes. After that, the surface of the air cathode with dimensions 200 mm × 40 mm × 2 mm, as shown in Figure 2, was impregnated with the prepared mixture using a brush. Microorganisms are the major component of MFC for treatment and electricity generation. Potter in 1911 demonstrated that yeast Saccharomyces cerevisiae and Bacillus coli provided suitable voltages for electricity generation [37-54]. So, for increasing the performance of the power output, knowledge of microorganism types from the viewpoint of properties, qualities, and quantities is needed.

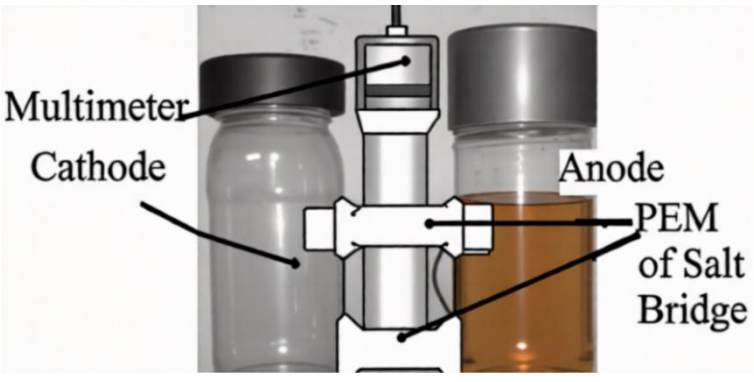

Figure 2. Preparing the cathode, salt bridge, and anode chambers.

2.5. Microbes used.

The major activation of bacteria is due to colonization of the anode electrode as a bio-catalyst to convert substrates and generate electricity. In Table 2, we used two microorganisms, including *Gluconobacter oxydans* [46] and *Geothrix fermentans* [47] bacteria in our MFC study.

Table 2. Different microorganisms are used in MFC.

No	Microorganisms	No	Microorganisms	No	Microorganisms
1	*Geobacter SPP* [38]	9	*Geothrix fermentas* [47]		*Erwinia dissolven* [53]
2	*Geobacter sulfurreducens* [39]	10	*Chlorella vugaris* [48]		*Lactobacillus plantarum* [53]
3	*Shewanella oneidensis* [40]	11	*Dunaliealla tertiolecta* [49]		*Paracoccus denitrificans* [53]
4	*Shewanella putrefaciens* [41]	12	*Scenedesmus obliquus* [49]		*Paracoccus pantotrophus*[54]
5	*Escherichia coli* [42]	13	*Chlorella pyrenoidosa* [50]		*Proteus vulgaris* [54]
6	*Clostridium butyricum* [43,44]	14	*Coriolus versicolor* [50]		*Proteus mirabilis* [54]
7	Pseudomonas a*eruginosa* [45,46]	15	*Agaricus meleagris* [51]		
8	*Gluconobacter oxydans* [46]	16	*Streptococcus lactis* [52]		

Geothrix fermentans is a rod-shaped, anaerobic bacterium measuring approximately 0.1 µm in diameter and 2–3 µm in length. Its cells occur either individually or in chains. This microorganism is commonly found in anaerobic aquatic sediments, including aquifers. As an anaerobic chemoorganotroph, *G. fermentans* is recognized for its ability to utilize ferric iron [Fe(III)] and other high-redox-potential metals as terminal electron acceptors. Additionally, it can metabolize a broad range of organic compounds as electron donors, contributing to its versatility in anaerobic environments. Research on metal reduction by *G. fermentans* has contributed to understanding more about the geochemical cycling of metals in the environment. This bacterium prefers acetate as an electron donor, but it can also utilize several other organic acids for growth, such as propionate and lactate. In addition to organic acids, *G. fermentans* can use fatty acids such as palmitate using Fe(III) as the sole electron acceptor. *G. fermentans* can also grow using other forms of iron and metals, such as manganese, but it shows a preference for iron or iron derivatives. Utilization of alternate electron acceptors by this organism depends on the electron donor present. It will also utilize nitrate (NO_3) and Mn(IV) as alternative electron acceptors when lactate is being used as the electron donor (Figure 3a). *Geothrix fermentans* is a rod-shaped, anaerobic bacterium measuring approximately 0.1 µm in diameter and 2–3 µm in length. Its cells occur either individually or in chains. This microorganism is commonly found in anaerobic aquatic sediments, including aquifers.

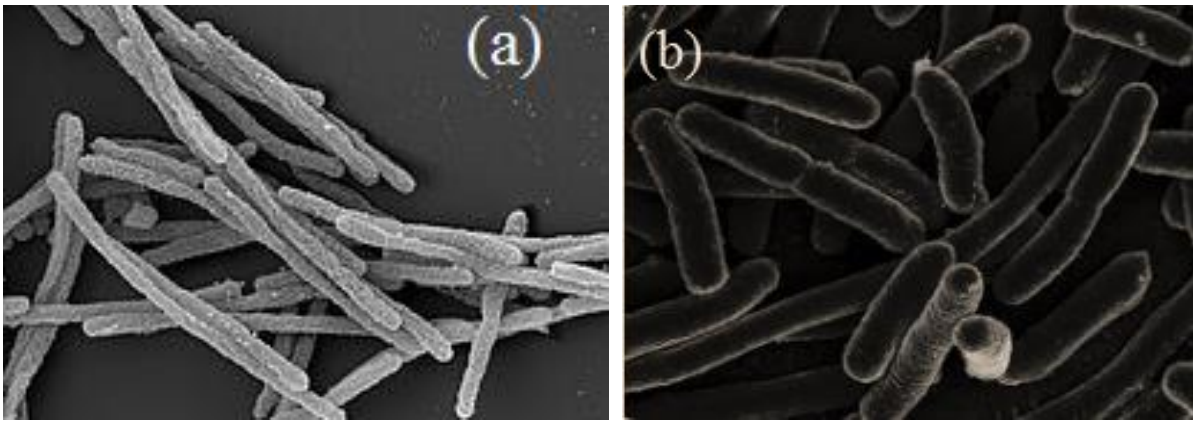

Figure 3. SEM of **(a)** *Gluconobacter oxydans*; **(b)** *Geothrix fermentans*.

As an anaerobic chemoorganotroph, *G. fermentans* is recognized for its ability to utilize ferric iron [Fe(III)] and other high-redox-potential metals as terminal electron acceptors.

Additionally, it can metabolize a broad range of organic compounds as electron donors, contributing to its versatility in anaerobic environments.

Gluconobacter is a genus of bacteria in the acetic acid bacteria family. They prefer sugar-rich environments, so are sometimes found as a spoilage organism in beer. They are not known to be pathogenic but can cause rot in apples and pears. They are used alone or with Acetobacter for microbial degradation of ethanol (Figure 3b)

2.6. Mass transfer and numerical analysis.

The air-cathode membrane, in the absence of an MFC, was first simulated using a steady-state two-dimensional model that incorporated bioelectrochemical kinetics along with mass, charge, and heat transfer. [12]. A schematic image of the modeling details is shown in Figure 4.

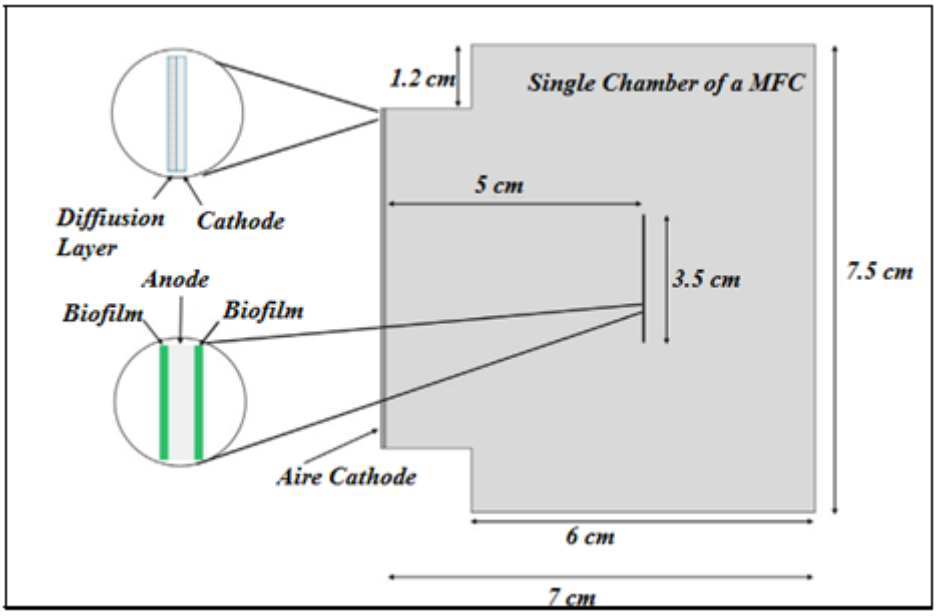

Figure 4. Schematic of a single chamber of MFC including an air cathode and biofilm.

The biofilm was assumed to be present on both sides of the anode and was modeled as a porous conductive matrix. The analyte was allowed to diffuse through the porous structure, where microorganisms oxidize the substrate, generating electrons and H^+ ions. The mathematical model was developed based on the following assumptions: The biofilm was represented as a solid porous conductive matrix with constant electrical conductivity and uniform pH. The added substrate was assumed to be uniformly mixed with the analyte, and substrate concentration gradients were considered to occur only within the biofilm. A concentration boundary layer was assumed to exist between the biofilm and the bulk analyte, exhibiting a linear substrate concentration profile. Based on equations 1 and 2, acetate and CO_2 stay in the anodic electrode and cannot diffuse from the anode chamber to the cathode chamber. Meanwhile, the air phase could not diffuse into the anodic chamber; thus, acetate is the only electron donor substrate remaining in the analyte. A biofilm within a porous matrix can generate electrons by oxidizing substrates and delivering them to the anodic chamber. Since the biomass ingredients, including bacteria and extracellular polymeric substances (EPS), constitute the solid conducting phase, only the liquid analyte phase containing the substrate solution enters the porous biofilm matrix and is oxidized by the bacteria. The biofilm matrix is similar to a porous surface, through two segregated currents, one for the solid phase and one

for the solution analyte phase. Obviously, electrons transfer from the solid state, and the ions from the electrolyte phase both obey Ohm's Law:

$$I = \sigma \nabla \varphi \; and \; i = \nabla I \quad (3)$$

Where "I" is the current density, σ is conductivity, "φ" is the potential, and "I" is the current source. The special current of electrons and ions in the case of porous chamber electrodes could be rearranged as:

$$i_s = \nabla I_s = \nabla(\sigma_{s,eff} \nabla \varphi_s \text{ and } i_l = \nabla I_l = \nabla(\sigma_{l,eff} \nabla \varphi_l \quad (4)$$

Where the subscripts "s" and "l" refer to the electrode phase and electrolyte phase, respectively. The effective amounts of conductivity (σ_{eff}) are calculated based on Bruggeman theory:

$$\sigma_{s,eff} = \in_s^{1.5} \sigma_s \text{ and } \sigma_{l,eff} = \in_l^{1.5} \sigma_l \quad (5)$$

Where $\in_s$ and $\in_l$ represent the volume fraction of the electrode and electrolyte phase, respectively, current density in the porous biofilm is a function of biomass and substrate concentrations, as well as a function of overpotential. By assuming substrate consumption through bacteria, which obeys Monod kinetics theory, the charge transfer kinetics at the anode could be rearranged as:

$$i_a = i_{0,a} \left(\frac{C_s}{C_s + K_{sa}}\right) C_x \exp\left(\frac{\alpha_a F \eta}{RT}\right) \quad (6)$$

Where, $C_s$is the concentration of the substrate, K_{sa} is half the maximum rate substrate concentration and C_x is the anodic bacteria concentration, α_a is anodic transfer coefficient, F is Faraday's constant, η is over potential, $i_{0,a}$ is the forward rate constant of the anode reaction at standard conditions[55,56]. Since the air-cathode used in the microbial fuel cell is a gas diffusion electrode (GDE) that is inert to charge transfer, the current density at the cathode can be described using a concentration-dependent Butler-Volmer function as follows:

$$i_c = i_{0,c}(\exp\left[\frac{\alpha_c F \eta}{RT}\right] - \frac{C_{O_2}}{C_{O_2(ref)}} \exp[\frac{-(1-\alpha_c)F\eta}{RT}] \quad (7)$$

Where, $i_{0,c}$ is the cathode reference exchange current density, CO_2 is the concentration of O_2, re, CO_2 (ref) is the reference concentration of O_2, α_c cathodic transfer coefficient. Since the overpotential (η) is a function of electrode potential, electrolyte potential, as well as the equilibrium potential of the charge transfer reaction, it could be rearranged as:

$$\eta = \varphi_s - \varphi_l - E_{eq} \quad (8)$$

The gradient of substrate in the biofilm can be formulated by:

$$\nabla D_{eff,a} \nabla C_s = \frac{a_a i_a}{nF} \quad (9)$$

Where, $D_{eff,a}$ is the effective diffusion coefficient, a_a is the active specific surface area of the anode, n (n=8-10) is the number of electrons involved in acetate (substrate) oxidation. Based on equation 10, since substrate cannot diffuse to the solid anodic chamber, a no-flux boundary condition is applied at the interface of the biofilm with the anodic electrode:

$$0 = D_{eff,a} \nabla C_s \quad (10)$$

The flux continuity condition (Eq. 11) was applied at the biofilm–analyte interface, assuming the presence of a concentration boundary layer with a thickness of "*L*" interface.

$$\frac{Da}{L}\left(C_{s,bulk} - C_s\right) = D_{eff,a}\nabla C_s \qquad (11)$$

Where, $C_{s,bulk}$ is the concentration, and *Da* is the diffusion coefficient of the substrate in the bulk analyte.

In addition, all tests were replicated several times with data normalization and exact control of the whole experiment.

3. Results and Discussion

3.1. Electricity production versus temperature and sample size.

Besides the experiment, we also supposed that the natural temperature and the largest possible sample size, with a larger percentage of organic matter, would generate the most electricity. We use thermal limits between 0°C and 40°C, experiments were accomplished for MFC's operating temperatures, 18°C, 23°C, 29°C, 37°C, and 40°C. Related parameters were estimated through experimental results at 23°C, 29°C, and 37°C. The accuracy of the model parameters was later established by comparing the experimental data for the other two MFCs, operating at 20°C and 40°C, with numerical predictions. In the first series of experiments, the independent variable being studied was the type of bacteria, *Gluconobacter oxydans* [46] and *Geothrix fermentans* [47] bacteria in related samples of the waste materials. We also fabricated our MFCs of these bacteria at room temperature (23°C) by measuring 3.0 cm × 3.0 cm × 4.0 cm dimensions for each type of sample. Therefore, 36 cm^3 volume of sample was used in each experiment for those four bacteria. Based on the sample size, a linear relationship can be observed between temperature effects and mechanistic aspects of microbial kinetics. For each sample, we measured electricity production using a digital multimeter within 5 minutes of MFC fabrication. Electricity production from several waste samples of various bacteria at 23°C is listed in Table 3.

Table 3. Electricity production from several waste samples of various bacteria at 23°C.

Waste sample	First trial (mV)	Second trial (mV)	Third trial (mV)	Medium
Gluconobacter oxydans	140	143	146	143
Geothrix fermentans	125	126	127	126

The measured amounts indicated that the MFC powered by the waste sample of the *Geothrix fermentans* has lower electricity production compared with the *Gluconobacter oxydans* sample.

Moreover, we completed several experiments through various percentages of organic matter in each of the waste samples. In the second category of the tests, we selected two temperatures (0°C versus 40°C) as an independent variable, while the dependent variable was the electricity production in each MFC. In addition, for a better comparison among the results, we also used the room temperature (23°C). We created MFCs using topsoil and measuring 3.0 cm × 3.0 cm × 4.0 cm for each temperature. Table 4 presents the results of the experiments and indicates that electricity production was greatest at 0°C and lowest at 40°C. In addition, we tested temperatures slightly above and below 0°C and 40°C. By this testing, we confirm that

an MFC cannot function at temperatures at or below −8°C or temperatures at or above 46°C. On the low temperature end, electricity production increases from −4°C to −1°C and to 0°C, and then decreases from 0°C to 4°C and then to 5°C. Interestingly, 0°C is a peak for two samples.

Table 4. Electricity production according to various temperature ranges for 4 samples.

Temperature (°C)	*Gluconobacter oxydans* (mV)	*Geothrix fermentans* (mV)
-8	None	None
-4	40	35
-1	88	75
0	155	144
4	89	70
5	80	69
18	90	81
23	143	126
29	70	65
37	64	58
40	48	38
43	18	11
46	None	None

According to the data in Table 4, the electricity production uniformly decreases from 29°C to 37°C, 40°C, and finally 43°C. Because we were unable to control the temperature in the enclosed environment, we were also unable to test performance at temperatures very close to −8°C or 46°C. Thus, for the purpose of this study, we considered −8°C and 46°C the thermal limits for MFC designing.

In the third range of experiments, we tested the independent amounts of the anode chamber size as well as the type of sample that fills the chamber, 10.0 cm × 10.0 cm × 13.0 cm versus 2.0 cm × 2.0 cm × 4.0 cm. Consequently, the MFC of medium size measuring 3.0 cm × 3.0 cm × 4.0 cm was selected and fabricated for comparison with other sizes. Table 5 presents the measured data for each category of our tests, and we found that electricity production increases with sample size, whereas, in contrast to our expectations, the efficiency of electricity production decreases with sample size. The volume of the largest MFC is 36.11 times the volume of the medium MFC, but the electricity production of the largest MFC for the *Gluconobacter oxydans* bacteria is approximately 1.13 times the electricity production of the medium MFC. Similarly, the volume of the medium MFC is 2.25 times the volume of the smallest MFC, but the electricity production of the medium MFC is only 1.24 times the electricity production of the smallest MFC. Therefore, we found that the amount of electricity production does not depend on the sample size and power in the various MFCs, directly. Although the electricity output increased with larger sample sizes, the efficiency gradually decreased; therefore, an important conclusion was that simply increasing the MFC size may not be very effective due to diminishing returns.

Table 5. Electricity production versus sample size.

Anode chamber size	*Gluconobacter oxydans* (mV)	*Geothrix fermentans* (mV)
2.0 × 2.0 × 4.0	122	116
3.0 × 3.0 × 4.0	143	126
10.0 × 10.0 × 13.0	170	155

3.2. Parameter estimation and model validation.

In this work, COMSOL software, which enables the running of coupled physics, was applied for numerical calculations. The program also serves as an application builder for physics applications. Several modules are available for COMSOL, categorized by application

areas: electrical, mechanical, fluid, chemical, multipurpose, and interfacing. [57]. COMSOL Multiphysics is a finite element analyzer, solver, and simulation software package for various physics and engineering applications, especially coupled phenomena and multi-physics. The software facilitates conventional physics-based user interfaces and coupled systems of partial differential equations (PDEs). COMSOL Multiphysics provides an IDE and unified workflow for electrical, mechanical, fluid, acoustics, and chemical applications. The Battery Design Module models and simulates the fundamental processes in the electrodes and electrolytes of batteries. These simulations may involve the transport of charged and neutral species, current conduction, fluid flow, heat transfer, and electrochemical reactions in porous electrodes. The chemical reaction engineering module provides a user interface for creating, inspecting, and editing model equations, kinetic expressions, functions, and variables for chemical systems.

Best-fit regression analysis based on the Nelder-Mead simplex optimization method was applied to determine the model parameters [11, 12]. The target function was established based on theoretical and experimental data for power density as a function of current density. Figure 5 shows the experimental and fitted polarization curves for MFCs operating at 23°C, 29°C, and 40°C from Table 4. Finally, COMSOL modeling parameters (boundary conditions, mesh size, solver type) were repeated in detail to ensure reproducibility.

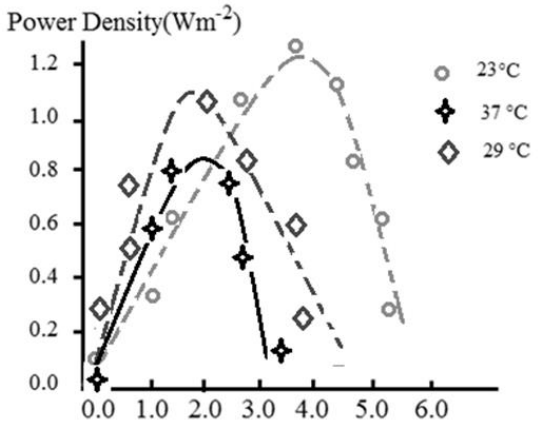

Figure 5. Power density vs current density for MFCs fabricated by *Gluconobacter oxydans* at 23°C, 29°C, and 37°C; experimental data are shown by solid separated marks, and numerical fitting is shown by a dotted line

3.3. Discussion.

As can be seen, the numerical technique could be predicted through accurate fitting with experimental data. The parameters obtained from fitting with the parameters that were obtained from experiments are also confirmed by other works. To prove our model's applicability in a wide range of temperatures, we used related parameter estimation compared with literature data. The CFD Module of COMSOL provides a dedicated physics interface for defining models of heat transfer in fluid and solid domains coupled to fluid flow in the fluid domain. We found that this model can be applied to predict the power density of MFCs operating at temperatures above and below, using numerical fitting. Consequently, there is good agreement between the numerically calculated and experimental data, confirming the applicability of the mathematical model over a wide range of temperatures. It is notable that the model has a strong potential to predict the nonlinear trend in power density as a function of various temperatures. From the experimental data, we found that the power density of MFCs at various temperatures increases linearly between 23°C and 37°C; however, as the operating temperature increases further, the power density begins to decrease. Both the experimental data

and the numerical analysis have shown approximately 5% decrease in maximum power density for an operating temperature of 40°C compared to 37°C. These results were related to the deviation amounts of the power increasing yielded during enhancement temperature from 23°C to 37°C. Recent researchers have developed the influence of temperature on MFC performance [58-63]. Liu *et al*. [58], Feng *et al*. [59], and Min *et al*. [49, 61] all confirmed a linear relationship in power output vs temperature in 20°C to 32°C, 20°C to 30°C, and 22°C to 30°C. Larrosa-Guerrero *et al*. [63] also found a similar increase in power density vs temperatures from 4°C to 35 °C. It is notable that in all previous studies, the maximum operating temperature is up to 35°C. We also studied the ionic strength, electrode spacing, type of bacterial culture in the anode biofilm, substrate composition, and its concentration. Obviously, an optimal correlation between power density and temperature cannot be achieved unless all other factors are accounted for simultaneously. This fact necessitates the use of numerical simulation to increase the efficiency of the electrical power in advanced MFCs. In addition, as shown in our previous work, the current steady-state investigation, which couples the energy balance with the effect of temperature, can also be suitable for considering the influence of other physical parameters. The scope and capability of the numerical calculations could be investigated by examining the power density as a function of ionic strength in the substrate solution and inter-electrode distance.

3.3.1. Ionic strength effects.

We studied electrolyte conductivity (σ_l) and the effect of ionic strength for the substrate solution on the MFC efficiency (equations 3-5). As can be seen in Figure 6, the highest power density initially increases linearly versus electrolyte conductivity between 0.12 W m^{-2} at $\sigma_l = 1e^{-4}$ Sm^{-1} to 1.1 W m^{-2} for $\sigma_l = 1e^{-2}$ Sm^{-1}.

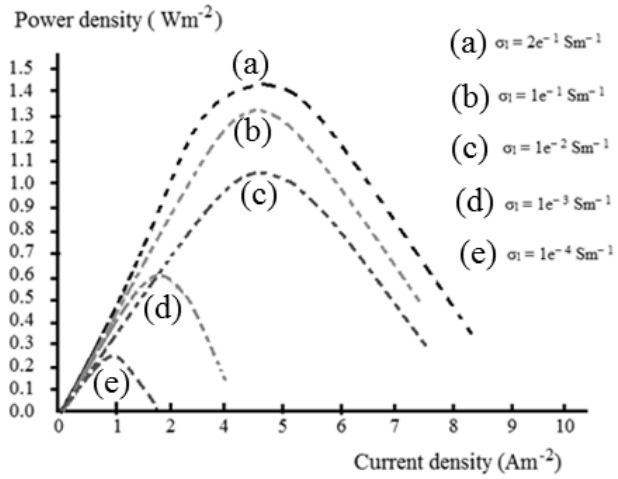

Figure 6. Power density of the *Gluconobacter oxydans* system in various conductivities vs current density.

Then, by enhancing conductivity, the power density gradually decreases towards $\sigma_l = 2e^{-1}$ Sm^{-1}. Since the conductivity shows the rate of ion transfer, higher conductivity causes ionic conduction, consequently reducing the Ohmic losses and power output of the MFCs. These results confirm our experimental data on the power density of the ionic strength from several bacterial substrates, where the increase in conductivity does not result in any further improvement in power density. In Table 6, the Ionic strength effects for *Gluconobacter oxydans* and *Geothrix fermentans* have been listed, both experimental and numerical calculations.

Table 6. Electricity production from several Waste samples of various bacteria at 23°C.

Waste sample/distance		Electrolyte conductivity (σ_l) with power density = 1.2 Wm^{-2}				
		$2e^{-1}\,Sm^{-1}$	$1e^{-1}\,Sm^{-1}$	$1e^{-2}\,Sm^{-1}$	$1e^{-3}\,Sm^{-1}$	$1e^{-4}Sm^{-1}$
Gluconobacter oxydans	experimental	1.38	1.27	1.02	0.61	0.21
	numerical	1.34	1.24	0.94	0.63	0.24
Geothrix fermentans	Experimental	1.33	1.12	0.92	0.62	0.19
	numerical	1.27	1.09	0.83	0.57	0.20

3.3.2. Electrode chambers structural size effect.

The effect of the electrode chambers' structural size and the inter-electrode distance between anode and cathode has been investigated for *Gluconobacter oxydans* and *Geothrix fermentans* bacteria. Inter-electrode distances were varied from 1 cm to 5cm. In all items, maximum power density increases as the distance between the two electrodes is decreased. Based on our experimental results and numerical studies, in general, as the inter-electrode distance decreased, the internal resistance also decreased. The effect of electrode distance also depends on the ionic strength change of the solution. It was observed that when electrolytes with conductivities more than 0.02 S m^{-1} were used, decreasing the electrode spacing does not result in any significant gain in power output, but power output changes with electrolyte conductivity smaller than 0.02 S m^{-1}. With electrolyte conductivity equal to 0.01 S m^{-1}, we calculated approximately 10% increase in power output as the distance increased from 5 cm to 1 cm. Moreover, using an electrolyte with a weak ionic strength equal to $\sigma_l = 1e^{-4}$ S m^{-1}, maximum power density changes from 0.7 Wm^{-2} towards 1.3 Wm^{-2} during reducing distance from 5 cm to 1 cm (Figure 7).

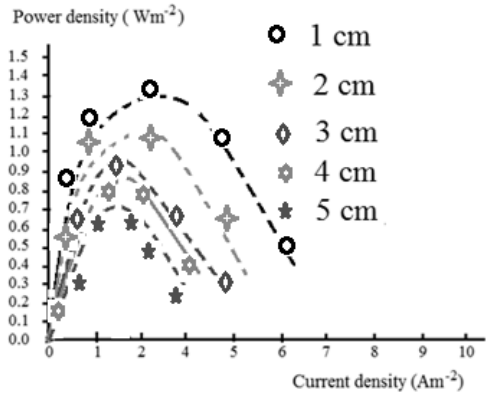

Figure 7. Power density of *Gluconobacter oxydans* system in various distances vs current density with electrolyte conductivity = 0.01 S m^{-1}, experimental data are shown by solid separated marks, and numerical fitting is shown by a dotted line.

In Table 7, the distance effect for *Gluconobacter oxydans* and *Geothrix fermentans* has been listed, both experimental and numerical calculations.

Table 7. Electricity production from several Waste samples of various bacteria at 23°C.

Waste sample/distance		Power density(Wm^{-2}) with conductivity = 0.01 S m^{-1} and $\sigma_l = 1e^{-4}$ S m^{-1}				
		1 cm	2 cm	3 cm	4 cm	5 cm
Gluconobacter oxydans	experimental	1.3	1.1	0.95	0.85	0.7
	numerical	1.35	0.9	0.9	0.80	0.75
Geothrix fermentans	experimental	1.25	1.05	0.90	0.8	0.65
	numerical	1.2	1.0	0.85	0.75	0.7

3.3.3. Analysis, replicates, or statistical interpretation.

Several electrodes were linked in parallel in order to increase their surface area, thereby increasing current, as well as for the analysis and performance evaluation. At first, distilled

water was poured into the cells and initial readings taken, then the water was emptied, and the cells were filled with *Geothrix fermentans* and *Gluconobacter oxydans* in parallel for analyzing and comparing microbial electroactivity. Variations in pH, voltage, and currents were monitored and recorded. The same substrate composition was used throughout this research work. In addition, data collected after sampling and the readings were analyzed in SPSS, and statistical analyses such as descriptive statistics, correlation, and regression were performed, yielding a predicted average voltage from the regression equation with RMSE=0.99.

4. Conclusions

A numerical method was developed to explain the nonlinear temperature dependence of microbial fuel cell (MFC) efficiency. The results demonstrate that system parameters are strongly interdependent and must be evaluated collectively to achieve a realistic assessment of MFC performance. Owing to its rapid convergence and computational efficiency, the proposed mathematical model is applicable to various MFC configurations and can also be extended to time-dependent analyses of dynamic efficiency. Beyond temperature effects, the model can be employed to investigate other key parameters, including ionic strength, reactor dimensions, ionic conductivity, and electronic current density. Future studies may focus on electroactive microorganisms that directly convert organic substrates into electricity while simultaneously oxidizing them to carbon dioxide. The use of MFCs in wastewater treatment offers significant advantages, including efficient energy recovery from organic matter, operation at mesophilic conditions, and the absence of toxic by-products. Additionally, wastewater can serve as a substrate for electricity generation, partially offsetting treatment costs. Despite the environmental importance of microbial pollutant removal, limited contact between contaminants and microorganisms remains a major constraint. Therefore, careful evaluation of residual contaminant levels and system efficiency is required. In this context, transition metal oxide nanocatalysts may enhance system performance and pollutant degradation.

Author Contributions

Conceptualization, M.M.; methodology, M.M. and F.M.; software, S.M.; validation, M.M. and S.M.; formal analysis, F.M and S.M.; investigation, M.M.; resources, Y.S, M.R.; data curation, S.M and Y.S.; writing—original draft preparation, M.M, F.M,S.M.; writing—review and editing, M.M.; visualization, Y.S, M.R.; supervision, M.M.; project administration, M.M.; All authors have read and agreed to the published version of the manuscript.

Institutional Review Board Statement

Not applicable.

Informed Consent Statement

Not applicable.

Data Availability Statement

Data supporting the findings of this study are available upon reasonable request from the corresponding author.

Funding

This research received no funding.

Acknowledgments

The authors thank the IAU University for providing the lab instrument, material, and devices.

Conflicts of Interest

The authors declare no conflict of interest.

References

1. Al-Asheh, S.; Al-Assaf, Y.; Aidan, A. Single-chamber microbial fuel cells' behavior at different operational scenarios.*Energies* **2020**, *13*, 5458, https://doi.org/10.3390/en13205458.
2. Kiaeenajad, A.; Moqtaderi, H.; Mahmoodi, N.; Maerufi, S.; Design and Construction of a Microbial Fuel Cell for Electricity Generation from Municipal Wastewater Using Industrial Vinasse as Substrate. *Mod. Mech. Eng.* **2020**, *20*, 2403-2412.
3. Ni, H.; Wang, K.; Lv, S.; Wang, X.; Zhuo, L.; Zhang, J. Effects of concentration variations on the performance and microbial community in microbial fuel cell using swine wastewater. *Energies* **2020**, *13*, 2231, https://doi.org/10.3390/en13092231.
4. Tan, S.M.; Ong, S.A.; Ho, L.N.; Wong, Y.S.; Thung, W.H.; Teoh, T.P. The reaction of wastewater treatment and power generation of single chamber microbial fuel cell against substrate concentration and anode distributions. *J. Environ. Health Sci. Eng*. **2020**, *18*, 793-807, https://doi.org/10.1007/s40201-020-00504-w.
5. Saravanan, P. Microbial fuel cell: a prospective sustainable solution for energy and environmental crisis, *Int. J. Biosens. Bioelectron.* **2018**, *4*, 191–193, https://doi.org/10.15406/ijbsbe.2018.04.00124.
6. Yuan, H.; Hou, Y.; Abu-Reesh, I.M.; Chen, J.; He, Z. Oxygen reduction reaction catalysts used in microbial fuel cells for energy-efficient wastewater treatment: a review. *Mater. Horiz.* **2016**, *3*, 382–401, https://doi.org/10.1039/c6mh00093b.
7. Kalathil, S.; Nguyen, V.H; Shim, J.J.; Khan, M.M.; Lee, J.; Cho, M.H. Enhanced performance of a microbial fuel cell using CNT/MnO_2 nanocomposite as a bio anode material. *J. Nanosci. Nanotechnol*. **2013**, *13*, 7712–7716, https://doi.org/10.1166/jnn.2013.7832.
8. Gabisa, E.W.; Gheewala, S.H. Potential of bio-energy production in Ethiopia based on available biomass residues. *Biomass Bioenergy* **2018**, *111*, 77–87, https://doi.org/10.1016/j.biombioe.2018.02.009.
9. Mollaamin, F.; Monajjemi, M. Graphene-based resistant sensor decorated with Mn, Co, Cu for nitric oxide detection: Langmuir adsorption & DFT method. *Sensor Review*, **2023**, *43*, 266–279. https://doi.org/10.1108/SR-03-2023-0040
10. Monajjemi, M.; Mollaamin, F.; Shahriari, S.; Khlaj, Z.; Sakhaeinia, H.; Alihosseini, A. Interaction of Nano-Boron Nitride Sheets with Electrodes in Lithium Ion Battery for Increasing Voltage and Amperage. *Russ. J. Phys. Chem. B* **2024**, *18*, 1090–1112, https://doi.org/10.1134/S1990793124700465.
11. Monajjemi, M.; Mohammadi, S.; Shahriari, S.; Mollaamin, F, Experimental and Theoretical Studies of ZnO Nanotubes: an Approach to Chemical Physics Characterization of ZnONTs, Including Morphology, Piezoelectric, and Density of States. *Russ. J. Phys. Chem. B* **2024**, *18*, 308–324, https://doi.org/10.1134/S1990793124010342.
12. Gadkari, S.; Gu, S.; Sadhukhan, J. Two-dimensional mathematical model of an air-cathode microbial fuel cell with graphite fiber brush anode. *J. Power Sources* **2019**, *441*, 227145, https://doi.org/10.1016/j.jpowsour.2019.227145.
13. Shahriari, S.; Soofi, N.S.; Farzi, F.; Attarikhasraghi, N.; Khosravi, S.; Babaei Tuskiee, B.B.; Esmkhani, R.; Monajjemi, M. Interaction of nano-boron nitride/graphene sheets with anode lithium ion battery. *J. Comput. Theor. Nanosci.* **2016,** *13*, 3070-3082.
14. Evelyn, E.; Saputra, A.; Amri, A.; Marshall, P. Gostomski. Reaction kinetics for microbial-reduced mediator in an ethanol-fed microbial fuel cell. *MATEC Web Conf.* **2019**, *276*, 06010, https://doi.org/10.1051/matecconf/201927606010.

15. Worku, A.; Tefera, N.; Kloos, H.; Benor, S. Bioremediation of brewery wastewater using hydroponics planted with vetiver grass in Addis Ababa, Ethiopia. *Bioresour. Bioprocess.* **2018**, *5*, 39, https://doi.org/10.1186/s40643-018-0225-5.
16. Chen, J.; Wang, Y.; He, X.; Xu, S.; Fang, M.; Zhao, X.; Shang, Y. Electrochemical properties of MnO2 nanorods as anode materials for lithium ion batteries. *Electrochim. Acta* **2014**, *142*, 152–156, https://doi.org/10.1016/j.electacta.2014.07.089.
17. Jia, M.; Zhang, Z.; Li, J.; Ma, X.; Chen, L.; Yang, X.; Molecular, P.A. Imprinting technology for microorganism analysis. *TrAC – Trends Anal. Chem.* **2018**, *106*, 190–201, https://doi.org/10.1016/j.trac.2018.07.011.
18. Aryal, N.; Ammam, F.; Patil, S.A.; Pant, D. An overview of cathode materials for microbial electrosynthesis of chemicals from carbon dioxide. *Green Chem.* **2017**, *19*, 5748–5760, https://doi.org/10.1039/c7gc01801k.
19. Vidali, M.; Bioremediation. An overview. *Pure Appl. Chem.* **2001**, *73*, 1163–1172, https://doi.org/10.1351/pac200173071163.
20. Santoro, C.; Arbizzani, C.; Erable, B.; Ieropoulos, I.; Microbial fuel cells: From fundamentals to applications. A review. *J. Power Sources* **2017**, *356*, 225–244, https://doi.org/10.1016/j.jpowsour.2017.03.109.
21. Monajjemi, M.; Yamola, H.; Mollaamin, F. Study of Bio-nano Interaction Outlook of Amino Acids on Single-walled Carbon Nanotubes. *Fuller. Nanotub. Carbon Nanostruct.* **2014**, *22*, 595–603, https://doi.org/10.1080/1536383X.2012.702163.
22. Cao, C.; Wang, H.; Liu, W.; Liao, X.; Li, L. Nafion membranes as electrolyte and separator for sodium-ion battery. *Int. J. Hydrog. Energy* **2014**, *39*, 16110-16115, https://doi.org/10.1016/j.ijhydene.2013.12.119.
23. Koók, L.; Nemestóthy, N.; Bélafi-Bakó, K.; Bakonyi, P. Treatment of dark fermentative H_2 production effluents by microbial fuel cells: A tutorial review on promising operational strategies and practices. *Int. J. Hydrog. Energy* **2021**, *46*, 5556–5569, https://doi.org/10.1016/j.ijhydene.2020.11.084.
24. Zuo, Y.; Cheng, S.; Logan, B.E. Ion exchange membrane cathodes for scalable microbial fuel cells. *Environ. Sci. Technol.* **2008**, *4218*, 6967–6972, https://doi.org/10.1021/es801055r.
25. Thomas, O.D.; Soo, K.J.W.Y.; Peckham, T.J.; Kulkarni, M.P.; Holdcroft, S. A Stable Hydroxide-Conducting Polymer. *J. Am. Chem. Soc.* **2012**, *134*, 10753–10756, https://doi.org/10.1021/ja303067t.
26. Hassan, N.U.; Motyka, E.; Kweder, J.; Ganesan, P.; Brechin, B.; Zulevi, B.; Col ón-Mercado, H.R.; Kohl, P.A.; Mustain, W.E. Effect of porous transport layer properties on the anode electrode in anion exchange membrane electrolyzers. *J. Power Sources* **2023**, *555*, 232371, http://dx.doi.org/10.2139/ssrn.4219578.
27. Wang, J.; Zhao, Y.; Setzler, B.P.; Rojas-Carbonell, S.; Ben Yehuda, C.; Amel, A.; Page, M.; Wang, L.; Hu, K.; Shi, L. Poly (aryl piperidinium) membranes and ionomers for hydroxide exchange membrane fuel cells. *Nat. Energy* **2019**, *4*, 392-398, https://doi.org/10.1038/s41560-019-0372-8.
28. Truong, V.M.; Yang, M.-K.; Yang, H. Functionalized Carbon Black Supported Silver (Ag/C) Catalysts in Cathode Electrode for Alkaline Anion Exchange Membrane Fuel Cells. *Int. J. Precis. Eng. Manuf.-Green Technol.* **2019**, *6*, 711–721, https://doi.org/10.1007/s40684-019-00123-3.
29. Lee, W-H.; Park, E.J.; Han, J.; Shin, D.W.; Kim, Y.S.; Bae, C. Poly(terphenylene) Anion Exchange Membranes: The Effect of Backbone Structure on Morphology and Membrane Property. *ACS Macro Lett.* **2017**, *6*, 566–570, https://doi.org/10.1021/acsmacrolett.7b00148.
30. Marinkas, A.; Struźyńska-Piron, I.; Lee, Y.; Lim, A.; Park, H.S.; Jang, J.H.; Kim, H.-J.; Kim, J.; Maljusch, A.; Conradi, O. Anion-conductive membranes based on 2-mesityl-benzimidazolium functionalised poly (2, 6-dimethyl-1, 4-phenylene oxide) and their use in alkaline water electrolysis. *Polymer* **2018**, *145*, 242-251, https://doi.org/10.1016/j.polymer.2018.05.008.
31. Santoro, C.; Lei, Y.; Li, B.; Cristiani, P. Power generation from wastewater using single chamber microbial fuel cells (MFCs) with platinum-free cathodes and pre-colonized anodes. *Biochem. Eng. J.* **2012**, *62*, 8–16, https://doi.org/10.1016/j.bej.2011.12.006.
32. Santoro, C.; Li, B.; Cristiani, P.; Squadrito, G. Power generation of microbial fuel cells (MFCs) with low cathodic platinum loading. *Int. J. Hydrogen Energy* **2013**, *38*, 692–700, https://doi.org/10.1016/j.ijhydene.2012.05.104.
33. Mollaamin, F.; Shahriari; Monajjemi, M. *Russ. J. Phys. Chem. B* **2014**, *18*, 398–418, https://doi.org/10.1134/S199079312402026X.

34. Baudler, A.; Schmidt, I.; Langner, M.; Greiner, A.; Schröder, U. Does it has to be carbon? Metal anodes in microbial fuel cells and related bioelectrochemical systems. *Energy Environ. Sci.* **2015**, *8*, 2048–2055, https://doi.org/10.1039/C5EE00866B.
35. Qiao, Y.; Li, C.M.; Bao, S.J.; Bao, Q.L. Carbon nanotube/polyaniline composite as anode material for microbial fuel cells. *J. Power Sources* **2007,** *170*, 79–84, https://doi.org/10.1016/j.jpowsour.2007.03.048.
36. Marshall, C.W.; Ross, D.E.; Fichot, E.B.; Norman, R.S.; May, H.D. Long-term operation of microbial electrosynthesis systems improves acetate production by autotrophic microbiomes. *Environ. Sci. Technol.* **2013**, *47*, 6023–6029, https://doi.org/10.1021/es400341b.
37. Jung, S.; Regan, J.M. Comparison of anode bacterial communities and performance in microbial fuel cells with different electron donors. *Appl. Microbiol. Biotechnol.* **2007**, *77*, 393–402, https://doi.org/10.1007/s00253-007-1162-y.
38. Mollaamin, F. Competitive Intracellular Hydrogen-Nanocarrier Among Aluminum, Carbon, or Silicon Implantation: a Novel Technology of Eco-Friendly Energy Storage using Research Density Functional Theory. *Russ. J. Phys. Chem. B* **2024**, *18*, 805–820, https://doi.org/10.1134/S1990793124700131.
39. Reguera, G.; Nevin, K.P.; Nicoll, J.S.; Covalla, S.F.; Woodard, T.L.; Lovley, D.R. Biofilm and nanowire production leads to increased current in Geobacter sulfurreducens fuel cells. *Appl. Environ. Microbiol.* **2006**, *72*, 7345–7348, https://doi.org/10.1128/AEM.01444-06.
40. Mollaamin, F.; Monajjemi, M. Electric and Magnetic Evaluation of Aluminum–Magnesium Nanoalloy Decorated with Germanium Through Heterocyclic Carbenes Adsorption: A Density Functional Theory Study. *Russ. J. Phys. Chem. B* **2023**, *17*, 658–672, https://doi.org/10.1134/S1990793123030223.
41. Kim, H.J.; Hyun, M.S.; Chang, I.S.; Kim, B.H. A microbial fuel cell type lactate biosensor using a metal-reducing bacterium, Shewanella putrefaciens. *J. Microbiol. Biotechnol.* **1999**, *9*, 365–367.
42. Mollaamin, F.; Monajjemi, M. Nanomaterials for Sustainable Energy in Hydrogen-Fuel Cell: Functionalization and Characterization of Carbon Nano-Semiconductors with Silicon, Germanium, Tin or Lead through Density Functional Theory Study. *Russ. J. Phys. Chem. B* **2024**, *18*, 607–623, https://doi.org/10.1134/S1990793124020271.
43. Monajjemi, M.; Mohammadi, S.; Shahriari, S.; Mollaamin, F. Experimental and Theoretical Studies of ZnO Nanotubes: an Approach to Chemical Physics Characterization of ZnONTs. Including Morphology, Piezoelectric, and Density of States. *Russ. J. Phys. Chem. B* **2024**, *18*, 308–324, https://doi.org/10.1134/S1990793124010342.
44. Rabaey, K.; Boon, N.; Höfte, M.; Verstraete,W. Microbial phenazine production enhances electron transfer in biofuel cells. *Environ. Sci. Technol.* **2005**, *39*, 3401–3408, https://doi.org/10.1021/es048563o.
45. Lee, S.A.; Choi, Y.; Jung, S.; Kim, S. Effect of initial carbon sources on the electrochemical detection of glucose by *Gluconobacter oxydans*. *Bioelectrochemistry* **2002**, *57*, 173–178, https://doi.org/10.1016/s1567-5394(02)00115-9.
46. Bond, D.R.; Lovley, D.R. Evidence for Involvement of an Electron Shuttle in Electricity Generation by *Geothrix fermentans* Evidence for Involvement of an Electron Shuttle in Electricity Generation by *Geothrix fermentans*. *Appl. Environ. Microbiol.* **2005**, *71*, 2186–2189, https://doi.org/10.1128/AEM.71.4.2186-2189.2005.
47. Zhang, Y.; Noori, J.S.; Angelidaki, I. Simultaneous organic carbon, nutrients removal and energy production in a photomicrobial fuel cell (PFC). *Energy Environ. Sci.* **2011**, *4*, 4340–4346, https://doi.org/10.1039/C1EE02089G.
48. Lakaniemi, A.M.; Tuovinen, O.H.; Puhakka, J.A. Production of electricity and butanol from microalgal biomass in microbial fuel cells. *Bioenergy Res.* **2012**, *5*, 481–491, https://doi.org/10.1007/s12155-012-9186-2.
49. Mollaamin, F.; Monajjemi, M., Molecular modelling framework of metal-organic clusters for conserving surfaces: Langmuir sorption through the TD-DFT/ONIOM approach. *Mol. Simul.* **2023**, *49*, 365–376, https://doi.org/10.1080/08927022.2022.2159996.
50. Ziaja-Sołtys, M.; Jaszek, M. Exploring the Anticancer Potential of *Coriolus versicolor* in Breast Cancer: A Review. *Curr. Issues Mol. Biol.* **2025**, *47*, 808, https://doi.org/10.3390/cimb47100808
51. Shen, N.; Yang, Y.P.; Yu, H.Q. A white-rot fungus is used as a biocathode to improve electricity production of a microbial fuel cell. *Appl. Energy* **2012**, *98*, 594–596, https://doi.org/10.1016/j.apenergy.2012.02.058.
52. Gal, I.; Schlesinger, O.; Amir, L.; Alfonta, L. Yeast surface Display of dehydrogenases in microbial fuel-cells. *Bioelectrochemistry* **2016**, *112*, 53–60, https://doi.org/10.1016/j.bioelechem.2016.07.006.

53. Vega, C.L.C.; Fernandez, I. Mediating Effect of Ferric Chelate Compounds in Microbial Fuel-Cells With Lactobacillus Plantarum. Streptococcus-Lactis, and Erwinia Dissolvens. *Bioelectrochem. Bioenerg*. **1987**, *17*, 217–222, https://doi.org/10.1016/0302-4598(87)80026-0.
54. Rabaey, K.; Van de Sompel, K.; Maignien, L.; Boon, N.; Aelterman, P.; Clauwaert, P.; Schamphelaire, L.D.; Pham, H.C.; Vermeulen, J.; Verhaege, M.; Lens, P.N.L.; Verstraete, W. Microbial fuel cells for sulfide removal. *Environ. Sci. Technol*. **2006**, *40*, *17*, 5218–5224, https://doi.org/10.1021/es060382u.
55. Yao, S.; He, Y.L.; Song, B.Y.; Li, X.Y. A two-dimensional, two-phase mass transport model for microbial fuel cells. *Electrochim. Acta* **2016,** *212*, 201 –211, https://doi.org/10.1016/j.electacta.2016.06.167.
56. Zeng, Y.; Choo, Y. F.; Kim, B.H.; Wu, P. Modelling and simulation of two-chamber microbial fuel cell. *J. Power Sources* **2010**, *195*, 79 –89, https://doi.org/10.1016/j.jpowsour.2009.06.101.
57. Gadkari, S.; Fidalgo, B.; Sai, G. Numerical investigation of microwave assisted pyrolysis of lignin. *Fuel Process. Technol*. **2017**, *156*, 473–484, https://doi.org/10.1016/j.fuproc.2016.10.012.
58. Liu, H.; Cheng, S.; Logan, B.E. Power generation in fed-batch microbial fuel cells as a function of ionic strength, temperature, and reactor configuration. *Environ. Sci. Technol*. **2005**, *39*, 5488 –5493, https://doi.org/10.1021/es050316c.
59. Feng, Y.; Wang, X.; Logan, B.E.; Lee, H. Brewery wastewater treatment using air cathode microbial fuel cells. *Appl. Microbiol. Biotechnol*. **2008**, *78*, 873–880, https://doi.org/10.1007/s00253-008-1360-2.
60. Patil, S.A.; Harnisch, F.; Kapadnis, B.; Schröder, U. Electroactive mixed culture biofilms in microbial bioelectrochemical systems: the role of temperature for biofilm formation and performance. *Biosens. Bioelectron*. **2010**, *26*, 803–808, https://doi.org/10.1016/j.bios.2010.06.019.
61. Min, B.; Román, O.B.; Angelidaki, I. Importance of temperature and anodic medium composition on microbial fuel cell (mfc) performance. *Biotechnol. Lett.* **2008**, *30*, 1213–1218, https://doi.org/10.1007/s10529-008-9687-4.
62. Lorenzo, M.D.; Curtis, T.P.; Head, I.M.; Scott, K. A single-chamber microbial fuel cell as a biosensor for wastewaters. *Water Res*. **2009**, *43*, 3145–3154, https://doi.org/10.1016/j.watres.2009.01.005.
63. Larrosa-Guerrero, A.; Scott, K.; Head, I.M.; Mateo, F.; Ginesta, A.; Hernández-Fernández, F.J.; Godinez, C. Effect of temperature on the performance of microbial fuel cells. *Fuel* **2010**, *89*, 3985–3994, https://doi.org/10.3303/CET1021078.

Publisher's Note & Disclaimer